European ECOSTRESS Hub 2

Algorithm and Theoretical Basis Document

Gross Primary Productivity (GPP)
Water Use Efficiency (WUE)

Prepared by	Kanishka Mallick, Ziyu Lin, Tian Hu, Patrik Hitzelberger and Yoanne Didry (LIST)

Reference	D1.2-ATBD-GPP-WUE
Issue	2
Revision	2
Date of Issue	2026-02-13
Status	Version 2.0
Document Type	Algorithm and Theoretical Basis Document GPP and WUE
Distribution	LIST, ESA

Dissemination level

Name	Affiliation
Zoltan Szantoi	ESA
Kaniska Mallick	LIST
Ziyu Lin	LIST
Tian Hu	LIST
Patrik Hitzelberger	LIST
Yoanne Didry	LIST
Public	

APPROVAL (Document Release Sheet)

Responsibility	Name / Affiliation	Signature	Date
ATBD Developer (PI)	Kaniska Mallick / LIST		
Developer	Ziyu Lin / LIST	N/A	N/A
Contributor	Tian Hu / LIST	N/A	N/A
Contributor	Yoanne Didry / LIST	N/A	N/A
Contributor	Patrik Hitzelberger / LIST	N/A	N/A
Approval	Zoltan Szantoi / ESA		
Distribution	Public		

CHANGE LOG

Issue	Revision	Date	Page	Author	Comment
1	0	2025-01-02		Mallick, Lin	Initial version
1	1	2025-02-28		Lin, Mallick	Revised version
2	2	2026-02-13		Hu	Revised version

List of Acronyms

Abbreviation	Full name
EEH2	European ECOSTRESS Hub Phase 2
LUE	Light Use Efficiency
WUE	Water Use Efficiency
GPP	Gross Primary Productivity
LUT	Look up table
LST	Land surface temperature
ET	Evapotranspiration
EF	Evaporative fraction
STIC	Surface Temperature Initiated Closure
VPD	Vapor pressure deficit
APAR	Absorbed photosynthetically active radiation
fAPAR	Fractional absorbed photosynthetically active radiation
LAI	Leaf Area Index
VPM	Vegetation Photosynthesis Model
CASA	Carnegie-Ames-Stanford approach
PAR	Photosynthetically Active Radiation
SIF	Solar-induced chlorophyll fluorescence
CLMS	Copernicus Global Land Monitoring Services
PFT	Plant Functional Type

Table of Contents

Executive Summary

The European ECOSTRESS Hub (EEH) is a vital part of the European Space Agency's Earth Observation Envelop Program (EOEP). This program focuses on the development and delivery of biogeophysical products related to ecosystem functioning at a continental scale. These products, essential for understanding the health and behaviour of ecosystems, are produced and delivered in a timely manner, with a significant emphasis on ECOSTRESS data. ECOSTRESS, which stands for Ecosystem Spaceborne Thermal Radiometer Experiment on Space Station, has been operational since its launch in August 2018. The satellite measures surface temperature and other thermal variables, enabling the study of ecosystem stress, water use efficiency, and vegetation health. The EEH makes use of the rich time series data from ECOSTRESS to create continuous and reliable insights into how ecosystems are responding to environmental changes and droughts across different land use over Europe and African continents.

Since July 2022, the EEH is providing data products of some of the essential ecosystem functioning variables Land Surface Temperature (LST) and evapotranspiration (ET) (as instantaneous latent heat flux, LE), and additional cloud mask (CM), which are generated every three to five days, multiple daytime hour (depending on ECOSTRESS acquisition), on a reliable basis.

Gross Primary Productivity (GPP) and Water Use Efficiency (WUE) are two highly significant ecosystem functioning products planned to be delivered at the end of Phase-2 of EEH. While GPP of an ecosystem is the total amount of carbon fixed during photosynthesis in a given period of time, WUE is defined as the amount of carbon assimilated as biomass or grain produced per unit of water used by the vegetation. The daily 70m GPP (gC m^{-2} day^{-1}) and WUE (gC m^{-2} mm^{-1}) will be calculated for Europe and Africa and made available to the user for all the ECOSTRESS acquisitions between 08/2018 – 12/2025. The daily 70m GPP Collection Version 1.0 product will be derived based on a coupled light use efficiency (LUE) and Surface Temperature Initiated Closure (STIC) model. The GPP model is driven by daily biotic metrics (i.e., CLMS leaf area index and top-of-canopy albedo dataset, LIS-CI-A1 clumping index, OCO-2 atmospheric CO_2 concentration) and instantaneous meteorological data (i.e., ERA-5 derived air temperature and vaper pressure deficit, CM-SAF photosynthetically active radiation, and EEH land surface temperature). The daily 70m WUE Collection Version 1.0 product will be derived based on the EEH2 70m daily GPP and ET product. This document gives a theoretical basis of the GPP and WUE retrieval, describes the algorithm, and its practical processing procedure.

.1 Background of the ATBD

In EEH2, daily 70m GPP and WUE Collection 70m Version 1.0 products will be derived across Europe and Africa from August 2018 to December 2025. The instantaneous GPP estimates are at the ECOSTRESS overpass time. To downscale GPP from instantaneous to daily scale, the daily GPP product is then weighted by daily and instantaneous ratio of Photosynthetically Active Radiation (PAR). Daily WUE product will be calculated as the ratio of daily ET to daily GPP. These products represent an advancement by incorporating diurnal variations in PAR—one of the key drivers of GPP variability. - while also eliminating the temporal mismatches between model estimates and satellite observations.

.2 General context – GPP

.2.1 Introduction and knowledge gaps

Precise estimation of Gross Primary Productivity (GPP) —the total carbon sequestered by plants through photosynthesis—is crucial for understanding the intricate dynamics between the terrestrial biosphere and the atmosphere under climate change. However, the direct measurement of GPP at a large scale remains impractical, necessitating a reliance on satellite-based modelling. Current large-scale daily GPP datasets, generally constructed from optical data or Solar-induced chlorophyll fluorescence (SIF) satellite imagery, typically operate at coarse resolutions ranging from 1 km to 0.05 arc-degrees. These datasets utilize daily average values from meteorological for model calibration, yet they do not adequately account for their diurnal fluctuations that affect daily GPP. As a result, these products are limited in their ability to capture fine-scale spatial and temporal variations in GPP. To enhance accuracy and applicability, particularly in heterogeneous landscapes and under diverse environmental conditions, there is an urgent need for higher resolution GPP products that account for diurnal variability and improve consistency between satellite retrievals and observations.

.2.2 Commonly used methodologies for satellite-based GPP estimation

To address the need for accurate and high-resolution GPP mapping at regional and global scales, various satellite-based methodologies have been developed. These approaches can be broadly categorized into three types: process-based models, data-driven models, and semi-empirical (hybrid) models.

Process-based models take a fully mechanistic approach, integrating remote sensing data with detailed physiological processes to simulate GPP. These models couple biogeochemical and biophysical processes such as photosynthesis, transpiration, radiative transfer, land-use change, and vegetation dynamics, reducing biases associated with oversimplifications. Examples include terrestrial biogeochemical models (TBMs) and dynamic global vegetation models (DGVMs). While these models provide detailed simulations of ecological processes for different biomes, they require extensive parameterization and high computational resources. As a result, their GPP products are often produced at coarse spatial resolution (0.05 arc-degree) to enhance computational efficiency.

Data-driven models leverage machine learning algorithms to estimate GPP based on empirical relationships between satellite data and ground-based measurements. Unlike process-based models, they do not rely on mechanistic assumptions and can capture complex interactions, such as non-linear response, between environmental variables and GPP. However, their black-box nature limits interpretability, and they require large amounts of high-quality data. In data-sparse regions, such as the tropics, these models often struggle with underfitting, reducing their reliability.

Semi-empirical models integrate elements of both process-based models and data-driven approaches, leveraging the strengths of both methodologies. A common example is the Light Use Efficiency (LUE) model, which estimates GPP based on the theoretical relationship between absorbed photosynthetically active radiation (APAR) and light use efficiency (LUE). Compared to purely process-based or data-driven methods, this approach offers a balance between computational efficiency and ecological realism, making them a promising approach for generating high-resolution GPP products across diverse landscapes.

.2.3 Light Use efficiency modeling

The Light Use Efficiency (LUE) model, introduced by Monteith (1972), assumes that the rate of photosynthetic production is proportional to the amount of absorbed PAR by leaves. Building on this foundational concept, the leaf level empirical relationship is further extended to the ecosystem level through the "big leaf assumption". This assumption simplifies the ecosystem, as observed from a satellite pixel to a uniform "big leaf" with consistent photosynthetic activity. This framework has been widely adopted for satellite-based GPP estimation, leading to the development of several advanced LUE models, such as CASA(Potter et al., 1993), MOD17 (Running et al., 2004) and VPM (Xiao et al., 2004).

Despite its widespread use, the traditional LUE model faces several limitations. The environmental constraints are also oversimplified, failing to capture carbon assimilation–transpiration trade-off. For example, the GPP does not always positively correlate to solar radiation at water limited regions such as savanna, shrubland, and grassland (Qiu et al., 2024). Particularly in tropical regions, the variation between different LUE model reaches up to 32 % (Cai et al., 2014), indicating the need for more comprehensive representation on the non-linear relationship in water-carbon trade off to reduce model uncertainties.

Apart from inherent model limitations, spatial and temporal scale mismatches between satellite data and ground measurements also impede the accurate retrieval of GPP from space. Temporally, satellite overpass times are typically around noon, which fails to capture the full diurnal cycle of photosynthesis. This temporal mismatch can introduce inaccuracies in GPP estimates, especially in regions experiencing significant water or heat stress (Qiu et al., 2024). In these areas, plants often exhibit an asymmetrical diurnal cycle of photosynthesis, further complicating accurate GPP estimation. Spatially, the high spatial resolution plays a crucial role in estimating GPP in mixed canopies or areas with partial forest cover (Vanikiotis et al., 2018). Moreover, coarse-resolution meteorological data frequently fail to account for the distinct effects of microclimatic conditions on plants (Ahl et al., 2004). This limitation in meteorological data further contributes to model uncertainties and reduces the accuracy of GPP estimates.

To address the abovementioned limitations of traditional LUE models, recent studies have proposed several advancements. These improvements aim to enhance the accuracy of GPP estimation by addressing issues related to water-carbon trade off, and spatial-temporal resolution mismatches. high-resolution satellite missions like ECOSTRESS provide enhanced temporal resolution and fine scale estimates of Land Surface Temperature (LST) and Evapotranspiration (ET), which can be integrated into GPP models to improve temporal representation of plant response. Additionally, improved spatial resolution of vegetation canopy matrices (e.g., fAPAR,

LAI) and species classification maps can better distinguish biotic controls in heterogeneous ecosystems (Kong et al., 2022).

.3 Proposed GPP Modelling in EEH

To better capture the trade-off between carbon assimilation and transpiration in GPP estimation, we propose a hybrid model that integrates the Light Use Efficiency (LUE) model with the Surface Temperature Initiated Closure (STIC)-based stomatal conductance model (Figure 1). This approach is capable of operating across any spatio-temporal scale, leveraging high-resolution satellite data to improve accuracy and spatial representation. The LUE framework captures the canopy response to diurnal light variation, making it particularly effective towards regions with high light variability. The STIC-based GPP model simulates the instantaneous stomata controls in response to thermal and water vaper, thus compensates the lack of mechanistic presentation of water and CO_2 response in conventional LUE model. Additionally, the hybrid model leverages high spatial resolution satellite data from ECOSTRESS and high temporal resolution data on hourly scale to eliminate the scale mismatch effects. The enhanced resolution allows for more accurate representation of photosynthetic efficiency in heterogeneous regions, such as mixed forest and savanna ecosystem.

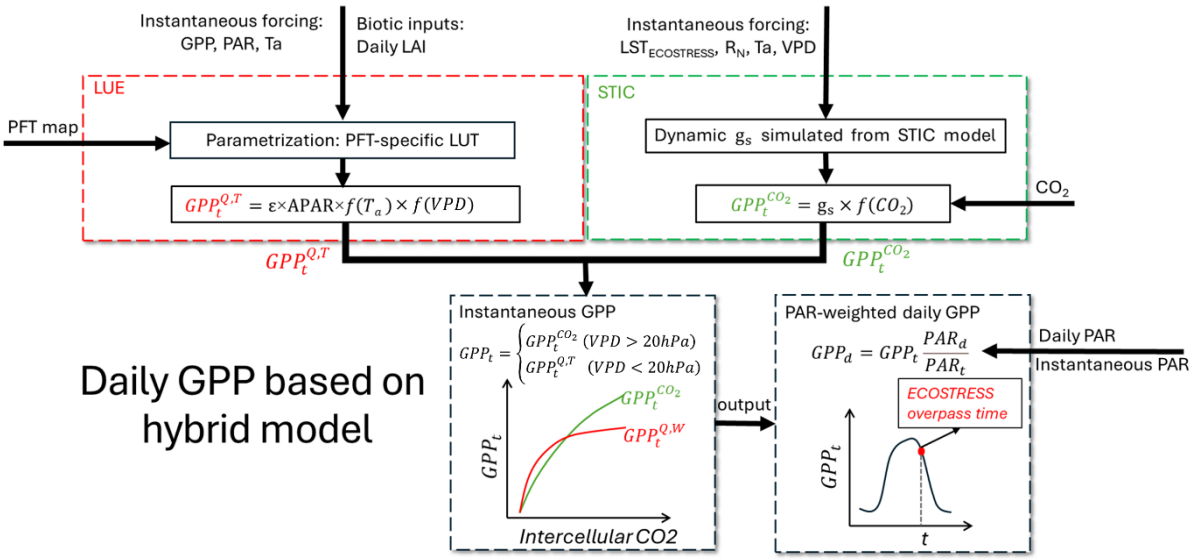

Figure 1. flow chart of daily GPP estimation

.3.1 Basic Structure of the coupled model with LUE and STIC model

While the LUE model effectively simulates the effects of light, water, and temperature on carbon assimilation rates, the empirical constraints could bring uncertainties, especially under water stress conditions. Conversely, the STIC stomata-based GPP model provides a physiologically realistic representation of stomatal regulation on plant water use by integrating thermal remote sensing information into the Penman-Monteith formulation. The structural characteristics of STIC enables estimating GPP from the instantaneous water use observed from space. However, it lacks explicit representation of GPP and its associated controls (i.e., temperature-mediated enzymatic control for reaction rate).

To address these limitations, we couple these two models to balance GPP estimation on carbon-water trade off. Thus, when marked stomatal closure begins at the empirical vapor pressure deficit (VPD) threshold of 20 hPa, we adopt the stomatal conductance-based method; otherwise, we use the LUE model:

$$GPP_t = \begin{cases} GPP_t^{CO_2} & (\text{VPD} > 20\text{hPa}) \\ GPP_t^{Q,T} & (\text{VPD} < 20\text{hPa}) \end{cases} \quad \text{Eq. (1)}$$

where:

$GPP_t^{Q,T}$ is LUE estimate constrained by temperature (T), and light(Q);

$GPP_t^{CO_2}$ is STIC estimate regulated by stomatal conductance and CO_2 availability.

Their units are in μmol CO_2 $m^{-2}s^{-1}$.

.3.2 LUE Model for simulating light-limited $GPP^{Q,T}$

The conventional LUE model is expressed as follows:

$$GPP^{Q,T} = \varepsilon_{max} \times PAR \times fAPAR \times T_s \times W_s \text{ , Eq. (2)}$$

$$T_s = \begin{cases} \frac{(T_a - T_{min})(T_a - T_{max})}{(T_a - T_{min})(T_a - T_{max}) - (T_a - T_{opt})^2} & (T_{min} < T_a < T_{max}) \\ 0 & (T_a < T_{min} \text{ or } T_a > T_{max}) \end{cases} \quad \text{Eq. (3)}$$

$$W_s = \begin{cases} 1 & (VPD < VPD_{min}) \\ \frac{VPD_{max} - VPD}{VPD_{max} - VPD_{min}} & (VPD_{min} < VPD < VPD_{max}) \\ 0 & (VPD > VPD_{max}) \end{cases} \quad \text{Eq. (4)}$$

where PAR denotes the photosynthetic active radiation (MJ m^{-2}), fAPAR denotes the fraction of PAR absorbed for photosynthesis (ranging from 0-1), and ε_{max} is optimum LUE without environmental stressors (CO_2 MJ^{-1}); T_s and W_s are the temperature and water downward-regulation scalar ranging from 0 to1. The temperature stress factor is calculated based on air temperature, where:T_a is the observed air temperature. T_{min}, T_{opt}, and T_{max} are the minimum, optimal, and maximum temperatures for photosynthesis, respectively. They will be parameterized for each PFT in the Look Up Table (LUT) (Table 2). W_s is based on VPD, with VPD_{min} of 9 hPa and VPD_{max} of 40 hPa.

.3.3 Using STIC model for simulating GPP^{CO_2}

Stomata control the balance of gases between the internal leaf environment and the external atmosphere, regulating CO_2 uptake for photosynthesis and water loss through transpiration. Assuming that the transport of CO_2 from the bulk air to the intercellular leaf space is limited by

both air-to-canopy surface diffusion and molecular diffusion through the stomata (i.e., aerodynamic conductance g_a and stomata conductance g_s), their total conductance g_t (Eq.6) controls the ecosystem carbon uptake and thus carbon assimilation. Using STIC model, we can simulate g_t directly from temperature and water vapor pressure. Linking the water vapor conductance to CO_2 conductance, we can derive the optimal GPP^{CO_2} (in μmol CO_2 $m^{-2}s^{-1}$) from atmospheric CO_2 concentration seasonality, expressed as follows.

$$GPP^{CO_2} = g_t \times c_g \times \Delta CO_2 \quad \text{Eq. (5)}$$

$$g_t = \frac{g_s \times g_a}{g_s + g_a} \quad \text{Eq. (6)}$$

$$\Delta CO_2 = \left(1 - \frac{c_i}{c_a}\right) \times \frac{c_i - \Gamma^*}{c_a + 2\Gamma^*} \times c_a \quad \text{Eq. (7)}$$

$$c_g = \frac{40.088}{1.6} \quad \text{Eq. (8)}$$

Where g_t, g_s and g_a are total conductance, stomata conductance and aerodynamic conductance for water vapor (H_2O) in unit of m s^{-1}, respectively. As byproduct of ET, the detailed derivations of g_s and g_a are given in STIC model Mallick et al. (2018). c_i (ppm) is the leaf-internal CO_2 concentration, c_a is the atmospheric CO_2 concentration, Γ* is the CO_2 compensation point estimated from Rubisco-limited temperature response (Bernacchi et al., 2001). As CO_2 diffuses more slowly through the stomata due to its larger molecular size and different chemical properties, the conductance is divided by 1.6 to account for the reduced diffusivity of H_2O-to-CO_2. Then we converted the conductance in m s^{-1} to molar units (mol m^{-2} s^{-1}) using the molar density of air, which is 40.088 mol m^{-3} under the ideal gas law and standard conditions (e.g., air pressure of 101.325 kPa and a temperature of 25°C).

.3.4 Daily product retrieved from instantaneous estimates

The daily GPP product will be retrieved from the instantaneous GPP_t at the ECOSTRESS overpass time, based on the PAR-weighted ratio of instantaneous and the daily values. The instantaneous and daily PAR data are derived from the CMSAF SARAH-3 dataset (Table 1). The daily WUE product will then be calculated out of the ratio between daily GPP and ET product of EEH. The calculations are expressed as follows.

$$GPP_d = m \times GPP_t \times \frac{PAR_d}{PAR_t} \quad \text{Eq. (9)}$$

$$WUE_d = \frac{GPP_d}{ET_d} \quad \text{Eq. (10)}$$

where GPP_d is in gC $m^{-2}day^{-1}$, ET is in mm day^{-1} and the WUE_d is in gC m^{-2}/mm H_2O. m is molar mass of carbon (i.e., 12 $\times 10^{-6}$ g μmol^{-1}) used for converting the GPP_d into mass unit of gC $m^{-2}day^{-1}$.

.4 Input data to be used

.4.1 Meteorological data

The instantaneous temperature data for running the GPP models were retrieved from the ERA-5 reanalysis meteorological dataset (https://www.ecmwf.int/en/forecasts/datasets/reanalysis-datasets/era5). The ERA-5 dataset provides gridded meteorological variables with a spatial resolution of 0.125 arc-degree (~12km) on an hourly basis. Air temperature at 2 m (Ta, ° C) and dew point temperature (Td, ° C) were used in this study. Then, we obtained vapor pressure deficit (VPD, Pa) from Ta and Td based on Clausius-Clapeyron relation.

The instantaneous and daily PAR data were sourced from CMSAF SARAH-3 product with a spatial resolution of 0.05 arc-degree (~5km) spanning Europe and Africa. This product was generated from the geostationary meteorological satellites.

The daily atmospheric CO_2 data was sourced from Orbiting Carbon Observatory-2 Goddard Earth Observing System (OCO-2 GEOS) Level 3 Carbon Dioxide assimilated dataset with a spatial resolution of 0.5×0.625 arc-degree.

.4.2 Satellite based biotic dataset

In this study, we used 2 biotic indies derived from the satellite data. The LAI were sourced from CLMS Collection 300m Version 1.0 based on PROBA-V and Sentinel-3/OLCI sensors (https://land.copernicus.eu/en/products). This dataset offers a full coverage of Europe and Africa, with a spatial resolution of 300m and a frequency of 10 days. Following the end of the PROBA-V mission in June 2020, the data transitioned to utilizing Sentinel-3 OLCI data with adjusted retrieval methodologies to maintain the consistency of the LAI time series. The annual 8-day canopy clumping index product were derived from MODIS. Due to the data not available after 2019, we used the average value 2016-2019 as a climatology input.

.4.3 Land use data

The GLC_FCS30D dataset provides annual global land cover maps with a spatial resolution of 30 meters, spanning the period from 1985 to 2022. GLC_FCS30D comprises 35 land-cover subcategories, with functional level vegetation categories including 9 PFTs: evergreen needleleaved forest (ENF), deciduous needleleaf forest (DNF), evergreen broadleaved forest (EBF), deciduous broadleaved forest (DBF), grassland (GRA), shrubland (SHR), cropland (CRO), wetland (WET) and tundra (TUN) (Zhang et al., 2024).

Table 1. remote sensing data used in the proposed hybrid model

Variables needed	Source name	Temporal resolution	Spatial resolution	Link	Purpose

Hourly incident PAR	CM-SAF	Hourly	0.05°	https://wui.cmsaf.eu/safira/action/viewProduktDetails?eid=22190_22473&fid=36	For estimating instantaneous APAR at the time of ECOSTRESS acquisition
Daily PAR	CM-SAF	Daily	0.05°	https://wui.cmsaf.eu/safira/action/viewProduktDetails?eid=22191_22474&fid=36	For estimating daily GPP
LAI, FCOVER	CLMS	10-day	300m	https://land.copernicus.eu/en/products/vegetation/fraction-of-absorbed-photosynthetically-active-radiation-v1-0-300m	For estimating APAR
g_s, g_a	ECOSTRESS Hub	Hourly	70m	Byproduct in EEH Phrase 2	For estimating CO_2 limited GPP
ET	ECOSTRESS Hub	Daily	70m	EEH Phrase 2	For estimating WUE
Temperature (air and dew point)	ERA-5	Hourly	1/4 °	https://cds.climate.copernicus.eu/datasets/reanalysis-era5-single-levels?tab=overview	For estimating VPD and Ta stressors in LUE model
Atmospheric CO2 (Ca)	OCO-2	Daily	0.5 ° x 0.625 °	https://disc.gsfc.nasa.gov/datasets/OCO2_GEOS_L3CO2_DAY_10r/summary	For estimating CO_2 limited GPP
LULC	GLC_FCS30D	Annual	30m	https://catalogue.ceda.ac.uk/uuid/b382ebe6679d44b8b0e68ea4ef4b701c/	For deriving PFT-specific look up table

.4.4 Ground carbon flux observations

The flux tower observations were sourced from 3 flux networks: FLUXNET2015 (FLUXNET, https://fluxnet.fluxdata.org/), European Flux Database Cluster (EFDC, http://www.europe-fluxdata.eu/), and AmeriFlux (https://ameriflux.lbl.gov/). We used the global dataset for the model parameterization, while the observations after 2018 at our study regions will be used for validation.

.4.5 Methodology

Step 1: Data harmonization

To ensure spatio-temporal consistency with ECOSTRESS observations, we harmonized our model inputs into 70m spatial resolution on daily and hourly temporal scale (Table 1). For biotic metrics and atmospheric CO_2 concentration which not significantly change diurnally, we used daily data as model inputs. For meteorological metrics, we used hourly data that are most closed to the ECOSTRESS overpass time as input. Spatially, the input data sourced from all databases were resampled into 70m resolution data based on the bilinear resample method. The annual 70m

land cover types were determined by referencing the 30m GLC_FCS30D data to identify the dominant type within each pixel, and areas without vegetation were excluded from the study analysis. For temporal harmonization, the biotic datasets with coarse temporal resolutions, including 10-day CLMS data and 8-day clumping index, were first smoothed by Savitzky-Golay filtering and then linearly interpolated into daily frequency (Chen et al., 2004).

Step 2: Model parametrization

The LUE was parameterized using a PFT-specific Look-Up Table (LUT) generated from remote sensing and flux tower observations during the growing season (Table 2). Specifically, we used the flux tower observed GPP as input to calibrate ε_{max} in LUE model for each PFT. The empirical T_{opt},T_{max},T_{min} for each PFT were estimated based on principles shown in Table 2. The start and end of growing season were determined based on the temperature and LAI value. Given the discrepancies between the footprint sizes of flux towers (ranging from 0.1 to 3 kilometers) and satellite observations (70 meters), heterogeneous sites were excluded from our study as per Chu et al. (2021). To ensure the representativeness of remote sensing data, we calculated the average LAI within a central area of 3 km × 3 km for forested sites (such as DBF, EBF, ENF, and MF) and 1 km × 1 km for other sites, aligning with previous studies (Zhou et al., 2016).

After parameterization, we estimate the instantaneous GPP at the ECOSTRESS overpass time *t* based on the coupled LUE and STIC model (Eq.1). The daily GPP were estimated from the PAR weighted method from instantaneous GPP (Eq. 9).

Table 2 PFT-specific look up table for LUE model

parameter	**unit**	**description**
ε_{max}	μmol CO_2 MJ^{-1}	Maximum light use efficiency
T_{opt}	°C	Optimal temperature at which $\varepsilon = \varepsilon_{max}$(at optimal VPD)
T_{max}	°C	Instantaneous maximum temperature at which $\varepsilon = 0$ (at any VPD)
T_{min}	°C	Instantaneous minimum temperature at which $\varepsilon = 0$ (at any VPD)

Step 3 Model evaluation

Based on flux tower observations, we first estimated the proposed coupled GPP_t model on the instantaneous estimates using the half hourly observations. Then we validated the daily GPP_d and WUE_d using daily observations. Finally, we employed a 5-fold cross-validation method to validate the model uncertainties for each PFT, using statistical metrics including the root mean square error (RMSE) and correlation coefficient (R).

.5 Reference

Ahl, D.E., Gower, S.T., Mackay, D.S., Burrows, S.N., Norman, J.M., Diak, G.R., 2004. Heterogeneity of light use efficiency in a northern Wisconsin forest: implications for modeling net primary production with remote sensing. Remote Sens. Environ. 93, 168–178. https://doi.org/10.1016/j.rse.2004.07.003

Bernacchi, C.J., Singsaas, E.L., Pimentel, C., Portis Jr, A.R., Long, S.P., 2001. Improved temperature response functions for models of Rubisco-limited photosynthesis. Plant, Cell & Environment 24, 253–259. https://doi.org/10.1111/j.1365-3040.2001.00668.x

Cai, W.W., Yuan, W.P., Liang, S.L., Liu, S.G., Dong, W.J., Chen, Y., Liu, D., Zhang, H.C., 2014. Large Differences in Terrestrial Vegetation Production Derived from Satellite-Based Light Use Efficiency Models. Remote Sens. 6, 8945–8965. https://doi.org/10.3390/rs6098945

Chen, J., Jönsson, Per., Tamura, M., Gu, Z., Matsushita, B., Eklundh, L., 2004. A simple method for reconstructing a high-quality NDVI time-series data set based on the Savitzky–Golay filter. Remote Sensing of Environment 91, 332–344. https://doi.org/10.1016/j.rse.2004.03.014

Chu, H., Luo, X., Ouyang, Z., Chan, W.S., Dengel, S., Biraud, S.C., Torn, M.S., Metzger, S., Kumar, J., Arain, M.A., Arkebauer, T.J., Baldocchi, D., Bernacchi, C., Billesbach, D., Black, T.A., Blanken, P.D., Bohrer, G., Bracho, R., Brown, S., Brunsell, N.A., Chen, J., Chen, X., Clark, K., Desai, A.R., Duman, T., Durden, D., Fares, S., Forbrich, I., Gamon, J.A., Gough, C.M., Griffis, T., Helbig, M., Hollinger, D., Humphreys, E., Ikawa, H., Iwata, H., Ju, Y., Knowles, J.F., Knox, S.H., Kobayashi, H., Kolb, T., Law, B., Lee, X., Litvak, M., Liu, H., Munger, J.W., Noormets, A., Novick, K., Oberbauer, S.F., Oechel, W., Oikawa, P., Papuga, S.A., Pendall, E., Prajapati, P., Prueger, J., Quinton, W.L., Richardson, A.D., Russell, E.S., Scott, R.L., Starr, G., Staebler, R., Stoy, P.C., Stuart-Haëntjens, E., Sonnentag, O., Sullivan, R.C., Suyker, A., Ueyama, M., Vargas, R., Wood, J.D., Zona, D., 2021. Representativeness of Eddy-Covariance flux footprints for areas surrounding AmeriFlux sites. Agricultural and Forest Meteorology 301–302, 108350. https://doi.org/10.1016/j.agrformet.2021.108350

Kong, J., Ryu, Y., Liu, J., Dechant, B., Rey-Sanchez, C., Shortt, R., Szutu, D., Verfaillie, J., Houborg, R., Baldocchi, D.D., 2022. Matching high resolution satellite data and flux tower footprints improves their agreement in photosynthesis estimates. Agricultural and Forest Meteorology 316, 108878. https://doi.org/10.1016/j.agrformet.2022.108878

Mallick, K., Toivonen, E., Trebs, I., Boegh, E., Cleverly, J., Eamus, D., Koivusalo, H., Drewry, D., Arndt, S.K., Griebel, A., Beringer, J., Garcia, M., 2018. Bridging Thermal Infrared Sensing and Physically-Based Evapotranspiration Modeling: From Theoretical Implementation to Validation Across an Aridity Gradient in Australian Ecosystems. Water Resources Research 54, 3409–3435. https://doi.org/10.1029/2017WR021357

Monteith, J.L., 1972. Solar Radiation and Productivity in Tropical Ecosystems. The Journal of Applied Ecology 9, 747. https://doi.org/10.2307/2401901

Potter, C.S., Randerson, J.T., Field, C.B., Matson, P.A., Vitousek, P.M., Mooney, H.A., Klooster, S.A., 1993. Terrestrial ecosystem production: A process model based on global satellite and surface data. Global Biogeochemical Cycles 7, 811–841. https://doi.org/10.1029/93gb02725

Qiu, R., Han, G., Li, X., Xiao, J., Liu, J., Wang, S., Li, S., Gong, W., 2024. Contrasting responses of relationship between solar-induced fluorescence and gross primary production to drought across aridity gradients. Remote Sensing of Environment 302, 113984. https://doi.org/10.1016/j.rse.2023.113984

Running, S.W., Nemani, R.R., Heinsch, F.A., Zhao, M., Reeves, M., Hashimoto, H., 2004. A Continuous Satellite-Derived Measure of Global Terrestrial Primary Production. BioScience 54, 547. https://doi.org/10.1641/0006-3568(2004)054[0547:acsmog]2.0.co;2

Vanikiotis, T., Stagakis, S., Kyparissis, A., 2018. Effects of satellite spatial resolution on Gross Primary Productivity estimation through Light Use Efficiency modeling, in: Themistocleous, K., Papadavid, G., Michaelides, S., Ambrosia, V., Hadjimitsis, D.G. (Eds.), Sixth International Conference on Remote Sensing and Geoinformation of the Environment, Proceedings of SPIE. Spie-Int Soc Optical Engineering, Bellingham. https://doi.org/10.1117/12.2326605

Xiao, X.M., Zhang, Q.Y., Braswell, B., Urbanski, S., Boles, S., Wofsy, S., Berrien, M., Ojima, D., 2004. Modeling gross primary production of temperate deciduous broadleaf forest using satellite images and climate data. Remote Sens. Environ. 91, 256–270. https://doi.org/10.1016/j.rse.2004.03.010

Zhang, X., Zhao, T., Xu, H., Liu, W., Wang, J., Chen, X., Liu, L., 2024. GLC_FCS30D: the first global 30 m land-cover dynamics monitoring product with a fine classification system for the period from 1985 to 2022 generated using dense-time-series Landsat imagery and the continuous change-detection method. Earth Syst. Sci. Data 16, 1353–1381. https://doi.org/10.5194/essd-16-1353-2024

Zhou, Y.L., Wu, X.C., Ju, W.M., Chen, J.M., Wang, S.Q., Wang, H.M., Yuan, W.P., Black, T.A., Jassal, R., Ibrom, A., Han, S.J., Yan, J.H., Margolis, H., Roupsard, O., Li, Y.N., Zhao, F.H., Kiely, G., Starr, G., Pavelka, M., Montagnani, L., Wohlfahrt, G., D'Odorico, P., Cook, D., Arain, M.A., Bonal, D., Beringer, J., Blanken, P.D., Loubet, B., Leclerc, M.Y., Matteucci, G., Nagy, Z., Olejnik, J., U, K.T.P., Varlagin, A., 2016. Global parameterization and validation of a two-leaf light use efficiency model for predicting gross primary production across FLUXNET sites. J. Geophys. Res.-Biogeosci. 121, 1045–1072. https://doi.org/10.1002/2014jg002876